LBL-19458

Lawrence Berkeley Laboratory
UNIVERSITY OF CALIFORNIA

APPLIED SCIENCE DIVISION

To be presented at the Spring Technical Meeting
of the Central States Section and Western States
Section of The Combustion Institute,
San Antonio, TX, April 22-23, 1985

ENERGY TRANSFER IN REACTIVE AND NONREACTIVE
H_2 + OH COLLISIONS

O. Rashed and N.J. Brown

April 1985

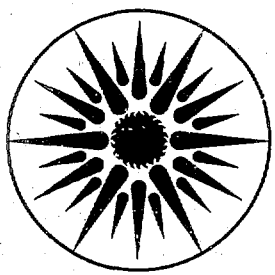

APPLIED SCIENCE
DIVISION

Prepared for the U.S. Department of Energy under Contract DE-AC03-76SF00098

LBL--19458

DE85 011156

ENERGY TRANSFER IN REACTIVE AND NON-REACTIVE H_2 + OH COLLISIONS

O. Rashed and N.J. Brown
Applied Science Division
Lawrence Berkeley Laboratory
University of California
Berkeley, California 94720

This work was supported by the Director, Office of Energy Research, Office of Basic Energy Science, Chemical Sciences Division of the U.S. Department of Energy under Contract No DE-AC-03-76SF00098

ABSTRACT

We have used the methods of quasi-classical dynamics to compute energy transfer properties of non-reactive and reactive H_2 + OH collisions. Energy transfer has been investigated as function of translational temperature, reagent rotational energy, and reagent vibrational energy. The energy transfer mechanism is complex with ten types of energy transfer possible, and evidence was found for all types. There is much more exchange between the translational degree of freedom and the H_2 vibrational degree of freedom than there is between translation and OH vibration. Translational energy is transferred to the rotational degrees of freedom of each molecule. There is a greater propensity for the transfer of translation to OH rotation than H_2 rotation. In reactive collisions, increases in reagent translational temperature predominantly appear as vibrational energy in the water molecule. Energy transfer in non-reactive and reactive collisions does not depend strongly on the initial angular momentum in either molecule. In non-reactive collisions, vibrational energy is transferred to translation, to the rotational degree of freedom of the same molecule, and to the rotational and vibrational degrees of freedom of the other molecule. In reactive collisions, the major effect of increasing the vibrational energy in reagent molecules is that, on the average, the vibrational energy of the reagents appears as product vibrational energy.

I. INTRODUCTION

Energy transfer is of fundamental importance in many elementary processes, e.g., chemical reactivity and collisional deactivation of excited states. While there has been considerable research effort devoted to the study of energy transfer in atom molecule systems[1-7], relatively little effort has been expended toward acquiring an understanding of the energy transfer phenomena in molecule-molecule collisions[8-14]. A major reason for the present state of affairs is that there are few potential energy surfaces available for the study of molecule-molecule collisions. A reasonable potential energy surface (PES) for the H_2 + OH system does exist, and this affords us an opportunity to investigate energy transfer in this system. This PES is the Rashed-Brown[15] modification of the analytical fit of Schatz-Elgersma[10] to the *ab initio* calculations of Walsh and Dunning[16].

In addition to energy transfer, collisions between H_2 and OH produce H_2O and H, and this bimolecular reaction is important in combustion systems. In hydrogen/oxygen flame systems this reaction appears to be the principal source of water at temperatures below those where partial equilibrium obtains[17]. In hydrocarbon/air flames at atmospheric pressure, it is the main source of water[18].

In a previous paper[15], we describe the effect of the energy distribution of the reagents on reactivity. Thermal rate coefficients were also computed at 1200 and 2000 K, and these agreed satisfactorily with experimentally determined values. In

this paper, the influence of translational energy, H_2 vibrational and rotational energy, and OH vibrational and rotational energy on energy transfer in non-reactive collisions and energy disposal in the products of reactive collisions is described.

II. MATHEMATICAL MODEL

The methods of quasi-classical dynamics discussed by several investigators are used in this study. The particular methods used to calculate energy transfer quantities are discussed in our previous paper. They will be briefly summarized here. The formalism incorporates three basis approximations: 1) the use of the Rashed-Brown modification to the Schatz-Elgersma analytical fit to the Walsh-Dunning potential surface, 2) the treatment of the dynamics with classical mechanics, and 3) the use of Monte Carlo averaging techniques to sample the phase space of the H_2 + OH system. The potential energy surface was modified to achieve the proper asymptotic behavior through removal of the spurious wells at large internuclear separations. The character of the potential surface near the saddle point geometry was retained since the analytical fit was particularly good in this region due to the high density of *ab initio* points. Monte Carlo techniques are used to determine the average collision characteristics for an ensemble of trajectories. For an ensemble of trajectories, we specify the translational temperature of the systems in kelvins, the initial vibrational energy of H_2, the initial rotational energy of H_2, the initial vibrational energy of OH, and the initial rotational energy of OH. All energies are expressed in

kcal/mol, and an ensemble is designated in the following manner: (T,v,J,v',J') where T designates the translational temperature, v and J designate the vibrational and rotational quantum numbers of H_2, and v' and J'are the quantum numbers associated with OH. The boundary conditions and integration procedure are previously described. For non-reactive trajectories, the final energy of each molecule was determined and this was partitioned into vibrational and rotational energy using the following relationships:

$$E_r^f = \min\left\{V_D(r) + \frac{J_r^f \cdot J_r^f}{2\mu r^2}\right\} - V_D(r_e) \tag{2.1}$$

and

$$E_v = E_m^f - E_r^f \tag{2.2}$$

where E_r^f is the final rotational energy, $V_D(r_e)$ is a Morse potential for the molecule in question, J_r^f is the final angular momentum of the molecule, r is the internuclear separation, μ is the reduced mass, E_v^f is the final vibrational energy, and E_m^f is the final molecular internal energy. The minimum of the effective potential was found using the Newton-Raphson iteration technique. The final rotational quantum number J^f was determined from

$$J^f = -\tfrac{1}{2} + \tfrac{1}{2}\left[1 + 4J_r^f \cdot J_r^f/\hbar^2\right]^{\frac{1}{2}} \tag{2.3}$$

and the final diatomic vibrational quantum number, v^f, was

evaluated from

$$v^f = -\tfrac{1}{2} + \frac{1}{\pi\hbar}\int_{r-}^{r+}\left\{2\mu\left[E_m{}^f - V_D(r) - \frac{J^f \cdot J^f}{2\mu r^2}\right]\right\}^{\nu_2} dr \qquad (2.4)$$

where r+ and r- are the turning points of the effective potential at the energy $E_m{}^f$. In addition to determining the energy distribution in each molecule, the final translational energy E_t, the orbital angular momentum L_o, and the scattering angle were determined for each non-reactive trajectory. All energies are expressed in kcal/mol and angular momenta are expressed in multiples of $\hbar$.

For reactive trajectories, the final molecular energy E_{HOH}, the final molecular angular momentum J_{HOH}, the angular momentum about the scattering center L_o, the final translational energy E_t, and the scattering angle were determined. Energy was not partitioned within the water molecule since the potential does not treat the H atoms in water as identical.

Energy transfer is described in terms of changes in translational energy, and the rotational and vibrational energy in each molecule by subtracting relevant values of the initial energy from the final values. Angular momentum changes are determined in a similar fashion. Average values per a (designated by a quantity enclosed in <>) of the various energy transfer quantities are computed for each ensemble of trajectories. Histograms of the various types of final energies in the system were computed for both non-reactive and reactive collisions in a given ensemble. Further understanding of the energy transfer mechanism is gained through the use of correlation coefficients,

which provide a measure of the relationship between two energy transfer quantities on a single collision basis. Correlation coefficients are defined as

$$\gamma_{xjyk} = \sum_{i=1}^{N} \frac{\Delta E_{xji}\Delta E_{yki} - <\Delta E_{xj}><\Delta E_{yk}>}{S_{xj}S_{yk}} \qquad (2.5)$$

where the subscripts x and y are used to represent t,r, or v indicating translational, rotational, and vibrational energy. The subscripts j and k each take on the values 1 or 2 with 1 designating the H_2 molecule and 2, OH. The quantity S_{xj} represents the standard deviation of the quantity E_{xj}, and N designates the number of non-reactive collisions in a given ensemble. Correlation coefficients assume values between -1.0 and +1.0. In the case of energy transfer, a negative value signifies that the loss of one quantity and gain of another are coupled in single collision events. Likewise a positive correlation coefficient indicates that both degrees of freedom either gain or lose energy in a single collision event. Correlation coefficients were computed for all types of energy transfer possible between the two molecules for non-reactive collisions.

III. RESULTS

The energy transfer mechanism is determined by examining the various average energy and angular momentum changes per collision, histograms of final energy and angular momentum distributions, and correlation coefficients. Energy transfer is investigated as a function of translational temperature, the

initial rotational energy in each molecule, and the initial vibrational energy in each molecule. The translational temperatures considered are 300 to 4000 K, with the majority of the calculations performed at 1200 and 2000 K. The initial value of the rotational quantum number is in the range 0-6 for H_2, and 0-7 for OH. The initial value of the vibrational quantum number for each molecule is in the range 0 to 4.

The precision in the energy transfer quantities is variable since the number of non-reactive (NNR) and the number of reactive trajectories (RT) varied from ensemble to ensemble. In general, the precision of quantities associated with non-reactive collisions was better. No conclusions have been drawn on differences less than the precision.

Some general trends are noted for energy transfer. The average translational energy transferred per collision is generally negative and less than 2.0 kcal/mol. The average change in angular momentum is generally a few units of $\hbar$, and the change is always positive for OH and positive for H_2 when the initial angular momentum is small. When both molecules are in v=0 or 1, the average vibrational energy change per collision is negative and less than 1 kcal/mol. In reactive collisions, the average scattering angle is $\sim$90 degrees, but the distribution of scattering angles for an ensemble of reactive trajectories is fairly uniform over the center-of-mass angles. The angular momentum in the system is evenly distributed between the H_2O molecule and the orbital angular momentum .

A. Translational Energy Dependence

The average energy transferred to the various degrees of freedom is summarized in Table I for ensembles having v_{HH}=1 and all other initial quantum numbers equal to 0. The initial value of the translational temperature is varied between 300 and 4000 K. There is a loss of translational and vibrational energy and a gain in the rotational energy of both molecules, and the losses and gains generally increase with translational temperature. Further insight into the energy transfer mechanism is provided by examining Table II where the ten correlation coefficients associated with the various modes of inter- and intra- molecular energy transfer in the system are tabulated. Correlation coefficients of magnitude less that 0.1 are treated as negligible. Looking down the various columns, there are ensembles where each of coefficients is in excess of 0.1. This indicates that the energy transfer mechanism is complex, involving all types of energy transfer. In fact, ten types of energy exchange are possible among the translational degree of freedom and the four molecular internal degrees of freedom. Energy transfer in diatom-diatom collisions is thus more complex than atom-molecule collisions. It is also important to recall that even though the average amount of energy transferred to a particular degree of freedom may indicate a net loss or gain mechanism, there are collisions in which this type of energy is lost and those in which energy is gained, unless of course, the degree of freedom had no energy deposited in it to begin with. The correlation coefficient for T-v exchange for H_2 remains large throughout the

table and does not vary systematically with temperature. At low temperature the r1-v1 correlation for H_2 is particularly strong indicating that v1-r1 transfer is an important mechanism for H_2 rotational energy gain. This mode of energy transfer becomes less important as the translational temperature increases, since T-r1 transfer increases with temperature. In these ensembles, OH has about 13 kcal/mol less vibrational energy than H_2. The major way OH gains rotational energy is through T-r2 transfer. Intermolecular internal energy transfer is unique to molecule-molecule collisions. The correlation coefficients for transfer of energy between the internal degrees of freedom of both molecules indicate that there is some H_2 vibrational energy transfer to the OH vibrational and rotational degrees of freedom. In collisions where OH gains vibrational energy, the source of energy is most likely H_2 vibration and not translational energy. The positive correlation for the two rotational degrees of freedom indicates a reasonably large number of collisions occur in which rotational energy is transferred to both molecules. This is a consequence of angular momentum conservation, which is less constrained in a two molecule system than in an atom-molecule system.

Examination of the histograms designating the distribution of various types of energy and angular momentum of ensembles, which differ only in the initial translational energy, provides additional information concerning the effect of translational energy on the energy transfer. Figure 1 is a histogram of ΔE_T for ensembles at 600, 1900, and 2000 K. The largest fraction of collisions in any bin are those that are nearly elastic. As the

temperature is increased, the distribution width increases, and the fraction of collisions which lose translational energy increases. Figs. 2 and 3 are histograms of the J^f of H_2 and OH, respectively at three translational temperatures. Again, the width of the distribution increases with temperature, and the effect is more profound for OH, which has a more asymmetric force field since the center-of-mass and center-of-charge are not coincident. At 1900 K and above, there are a number of collisions where OH experiences a large change in angular momentum. Histograms of ΔE_v at three different translational temperatures are shown in Figs. 4 and 5 for H_2 and OH, respectively. Many of the collisions are nearly elastic with respect to the excited vibrational degree of freedom of either molecule. The collisions tend to become more inelastic as the translational temperature increases, and the distribution width increases. The number of vibrational deactivating collisions increases more rapidly with temperature than the number of activating collisions. The molecule OH, which initially only has zero point energy, has a greater tendency to gain vibrational energy than H_2, which is excited to v=1. The OH gain most likely results from v1->v2 transfer.

The energy and angular momentum disposal in the products of reactive collisions are shown in Table III for ensembles that differ only in translational temperature. In general, there is a tendency for the relative translational energy, the angular momentum, and total energy of the H_2O molecule to increase with translational energy. These effects are shown more dramatically

in the next three figures. The translational energy distribution in the product system is shown in Fig. 6 for three values of the initial translational temperature. Although there is a gradual broadening of the distribution as the translational temperature is increased, the effect is not terribly profound, and thus accounts for the relatively small increase noted for E_T of the products. The translational energy of the products is plotted as a function of the reactant translational temperature in Fig. 7. Although the product translational energy does not depend monotonically on the reagent translational temperature, there is a tendency for it to increase. Fig. 8 is a plot of the H_2O energy as a function of reagent translational temperature, and it illustrates that the increase in translational energy in the reactants appears mostly as internal energy in the water molecule. The distribution of energies in the H_2O molecule as a function of translational temperature of the reagents is shown in Fig. 9. The effect of increased translational temperature increases the width of the distribution toward the higher energy side. It is interesting that the peak of the distribution is not effected by increases in translational temperature. The energy associated with the maximum population is approximately 38 kcal/mol, which is equal to the sum of the OH zero point energy, the H_2 energy of v=1, and the reaction exoergicity (~15 kcal/mol). The distribution of angular momentum in the water molecule for three different translational temperatures is shown in Fig. 10. Although the width of the distribution increases slightly, translational temperature increases in the reactants produce little effect on the angular momentum distribution of the

products. Since the angular momentum in water is relatively unaffected by the reactant translational temperature and the energy in water increases with it, the increase in E_{HOH} is an increase in vibrational energy.

B. Rotational Energy Dependence

In order to ascertain the effect of reagent rotation on energy transfer and energy disposal in products, ensembles where the translational temperature, the initial rotational energy of one molecule, and the vibrational energy of both molecules were fixed, and the rotational energy of the other molecule was varied, were compared. The collection of ensembles where both molecules were in v=0 is Case I and that for which H_2 was in v=1 is Case II.

In Case I, the average translational energy change per collision, which is usually negative, became more positive as the initial J of the molecule increased. This is illustrated in Fig. 11 where $\langle \Delta E_T \rangle$ is plotted as a function of the initial angular momentum of J_{OH} for ensembles at 1200 K with J_{HH} =4. The effect is more pronounced when J_{HH} is initially fixed and J_{OH} is allowed to vary. The average change in angular momentum per collision, which is always positive, decreases with initial J. This is shown in Fig. 12 where the change in J_{OH} per collision is plotted versus the initial value of J_{OH} for ensembles at 2000 K with the initial J_{HH} = 0. The same effect, of course, is noted for rotational energy. Vibrational energy transfer showed no systematic trend with the variation in initial rotational energy. On the average, both molecules lose vibrational energy and the

amount of energy lost in a set of ensembles with identical translational temperature and vibrational energy varies insignificantly.

All correlation coefficients were computed for the Case I ensembles. Most were small and negative with magnitudes less than 0.3, indicating that energy exchange among all degrees of freedom is possible, and that a dominant type does not prevail. The largest correlation coefficient for these ensembles was γ_{Tr2} indicating that OH rotational energy gain resulted from t->r energy transfer. Since the rotational energy transferred to OH decreases as the initial J_{OH} increases and the correlation coefficient for t->r remains constant, other modes of energy transfer to OH rotation must be important at small initial J_{OH}. At 1200 K, r->r transfer becomes more important as the initial J of one of the molecules increases since the correlation coefficient γ_{r1r2} for the intermolecular rotational energy transfer becomes more negative with increasing J. This type of energy transfer is a consequence of angular momentum conservation.

The energy transfer mechanism changes when H_2 is initially excited to v=1, Case II. The correlation coefficients γ_{Tv1} and γ_{r1v1} are quite large in magnitude. Some of the H_2 vibrational energy loss results in rotational energy gain. This most likely happens indirectly by, first transferring vibrational energy to translation and then transferring translational energy to rotation. For the Case II ensembles, the correlation coefficient γ_{Tr2} remains large but does not retain its dominant role in the

mechanism. Also the systematic trend note for γ_{r1r2} disappears.

Variation of the reagent rotational energy produced no systematic effects in the product energy disposal mechanism. The angular momentum in the product system is distributed between the H_2O molecule and the orbital angular momentum.

C. Vibrational Energy Dependence

In order to ascertain the effect of reagent vibration on energy transfer, collisions in ensembles having a fixed initial translational temperature, no initial angular momentum in either molecule, zero point vibrational energy in one molecule, with the initial vibrational energy of the other molecule allowed to varv between v=0 and 4, were compared. Energy transfer for non-reactive collisions of these ensembles are summarized in Table IV. As the vibrational energy of H_2 is increased, $\langle\Delta E_T\rangle$ decreases in magnitude(it is always negative), and $\langle\Delta J_{HH}\rangle$ and $\langle\Delta Er_{HH}\rangle$ increase. Similar behavior is observed for increasing v_{OH}. $\langle\Delta J_{OH}\rangle$ and $\langle\Delta Er_{OH}\rangle$ increase. At 1200 K $\langle\Delta E_T\rangle$ shows no systematic trend and at 2000 K decreases in magnitude with increasing v_{OH}. As the initial v for a given molecule increases, the average vibrational energy change for that molecule becomes more negative while the average vibrational energy change for the other molecule generally tends to become more positive. In general, OH does not lose as much vibrational energy as H_2.

Correlation coefficients for this collection of ensembles are listed in Table V, and these reveal some interesting aspects of the energy transfer mechanism. As v_{HH} is increased, γ_{r1v1} and γ_{Tv1} increase in magnitude and become more negative indicating

that vibrational energy of H_2 is transferred to translation and rotation. The coefficient γ_{Tr1} is often positive, indicating that rotational and translational energy gain often occurs in a given collision. It is likely that the v->r transfer is actually a two-step process occurring in a single collision whereby vibrational energy is first transferred to translation, and part of the translational energy is then transferred to rotation. Correlation coefficients involving OH are not particularly large except γ_{v1r2} and γ_{v1v2} which indicate that H_2 vibrational energy is transferred to OH vibration and rotation. The positive value of γ_{r1r2} indicates that both molecules often receive rotational energy in a single collision, which is a consequence of angular momentum conservation.

As v_{OH} is increased, we see the evolution of very complex energy transfer mechanism. The correlation coefficients indicate that there is energy transfer between OH vibrational energy and translational, OH rotational, H_2 rotational, and H_2 vibrational energy. Again there are collisions where both molecules gain rotational energy, and there is more transfer between translational energy and OH rotational energy than between translation and H_2 rotational energy. In general the OH vibrational degree of freedom is not as coupled to translation as the H_2 vibration is. This is responsible for the inability of OH vibrational energy to promote reactivity in the H_2 + OH system.

The effect of increasing vibrational energy in either reagent on the average energy disposal in products is shown for ensembles at 1200 and 2000 K in Table VI. The average

translational energy in the product system decreases slightly with v_{HH} and exhibits similar behavior with respect to v_{OH} at 2000 K. There is a tendency of $\langle \Delta J_{HOH} \rangle$ to increase with v_{HH}, but increasing v_{OH} has a negligible effect on it. The most interesting effect of increasing the vibrational energy of either reagent is shown in Fig. 13, where the average energy of the water molecule, $\langle E_{HOH} \rangle$, is plotted versus the vibrational energy of each reagent molecule at 1200 and 2000 K. The plots indicate that the increase $\langle E_{HOH} \rangle$ in going from v to v+1 quanta in either reagent is equal to $E_{v+1} - E_v$. Since there is only a small change in $\langle J_{HOH} \rangle$ with increasing v in either reagent, we know that, on the average, reagent vibrational energy appears as product vibrational energy. When both reagent molecules are vibrationally excited, average behavior is such that the vibrational energy of both reagents appears as product vibrational energy.

Additional information regarding energy disposal in the product system is obtained by examining histograms of product energy and angular momenta distributions. The effect of increasing v_{HH} can be illustrated by comparing histograms for the ensembles (0,0,0,0) and (4,0,0,0), while the effect of increasing v_{OH} can be determined from comparison of (0,0,0,0) and (0,0,4,0). The histograms of product translational energies are shown in Fig. 14. The translational energy distributions do not change significantly with v_{OH}, and the peak shifts to lower energies and the distribution width increases with v_{HH}. The product angular momentum histograms are shown in Fig. 15 and these are relatively unaffected by reagent vibrational energy. The most

interesting distributions are those of H_2O energies which are shown in Fig. 16. The minimum and maximum energy of each distribution increase with v, and the energy associated with the maximum population of the distribution is equal to the sum of vibrational energy of both molecules plus 10 kcal/mol. The maximum energy of the distribution is equal to the sum of the vibrational energies, the barrier, and the exoergicity. There are collisions which transfer an inordinate amount of energy into the product.

IV. SUMMARY AND CONCLUSIONS

We have used the methods of quasi-classical dynamics to compute energy transfer properties of non-reactive and reactive H_2 + OH collisions. The potential energy surface used was the Schatz-Elgersma fit to the ab initio Walsh-Dunning surface. Energy transfer has been investigated as function of translational temperature, reagent rotational energy, and reagent vibrational energy. The most important findings can be summarized as follows:

(1) The energy transfer mechanism is complex with ten types of energy transfer possible. Evidence was found for all types of energy transfer. Energy transfer in diatom-diatom collisions is far more complicated than A + BC collisions.

(2) There is much more exchange between the translational degree of freedom and the H_2 vibrational degree of freedom than there is between translation and OH vibration. Since translational energy is most effective in promoting reactivity in this system, and H_2 vibration couples strongly to it, this

accounts for the greater effectiveness of H_2 vibration in promoting reactivity than OH vibration.

(3) Translational energy is transferred to the rotational degrees of freedom of each molecule. There is a greater propensity for the transfer of translation to OH rotation than H_2 rotation.

(4) In reactive collisions, increases in reagent translational temperature predominantly appear as vibrational energy in the water molecule.

(5) The average change in translational energy per collision becomes more positive as the initial angular momentum in either reagent molecule increases, and the tendency for a molecule to gain angular momentum varies inversely with it initial angular momentum.

(6) Energy transfer in non-reactive and reactive collisions does not depend strongly on the initial angular momentum in either molecule. This is consistent with our interpretation of the dependence of reactivitity on reagent angular momentum. Rotational excitation of either or both reagent molecules suppresses reactivity by reducing the probability of achieving the proper reagent orientation required for reaction, and not by reducing energy in degrees of freedom, effective in promoting reaction.

(7) In non-reactive collisions, vibrational energy is

transferred to translation, to the rotational degree of freedom of the same molecule, and to the rotational and vibrational degrees of freedom of the other molecule. OH does not transfer vibrational energy as effectively as H_2.

(8) The major effect of increasing the vibrational energy in either or both reagent molecules is that, on the average, the vibrational energy of the reagents appears as product vibrational energy.

REFERENCES

1. J.T. Muckerman, J. Chem. Phys. **54**, 1155 (1971).

2. J.T. Muckerman, J. Chem. Phys. **56**, 2997 (1972).

3. N.C. Blais and D.G. Truhlar, J. Chem. Phys. **58**, 1090 (1973).

4. D.L. Thompson and N.C. Blais, J. Chem. Phys.**78**, 1335 (1983).

5. N.C. Blais and D.G. Truhlar, J. Phys. Chem. **86**, 638 (1982).

6. N.J. Brown, J. Chem. Phys. **60**, 2958 (1976).

7. N.J. Brown and J.A. Miller, J. Chem. Phys. **80**, 5568 (1984).

8. M.H. Mok and J.C. Polanyi, J. Chem. Phys. **53**, 4588 (1970).

9. G.C. Schatz, J. Chem Phys. **74**, 1133 (1981).

10. G.C. Schatz and H.Elgersma, Chem. Phys. Lett. **73**, 21 (1980).

11. G.C. Schatz and H. Elgersma in Potential Energy Surfaces and Dynamics Calculations, editted by D.G. Truhlar (Plenum, New York, 1981), p311.

12. N.J. Brown and D. M. Silver, J. Chem. Phys. **65**, 311 (1976).

13. N.J. Brown and D. M. Silver, J. Chem. Phys. **68**, 3607 (1978).

14. N.J. Brown and D. M. Silver, J. Chem. Phys. **72**, 3869 (1980).

15. O. Rashed and N.J. Brown, J. Chem. Phys. **82**, (1985).

16. S.P. Walsh and T.H. Dunning, J. Chem Phys. 72, 1303 (1980).

17. N.J. Brown, K.H. Eberius, R. M. Fristrom, K.H. Hoyermann, and H.Gg. Wagner, Combust Flame 33, 151 (1978).

18. J. Warnatz, in Combustion Chemistry, edited by W.C. Gardiner, Jr.(Springer-verlag, New York, 1984), p197.

LIST OF TABLES

Table I. Non-Reactive Trajectories

T	v_{HH}	J_{HH}	v_{OH}	J_{OH}	NNR	$\langle\Delta E_T\rangle$	$\langle\Delta J_{HH}\rangle$	$\langle\Delta J_{OH}\rangle$	$\langle\Delta E_{r_{HH}}\rangle$	$\langle\Delta E_{r_{OH}}\rangle$	$\langle\Delta E_{v_{HH}}\rangle$	$\langle\Delta E_{v_{OH}}\rangle$
300	1	0	0	0	4881	-.29	-.4	2.1	.03	.28	-.01	-.01
600	1	0	0	0	3699	-.40	-.6	2.7	.10	.51	-.20	-.01
800	1	0	0	0	1838	-.39	-.7	3.0	.21	.62	-.43	.00
1000	1	0	0	0	1149	-.43	-.9	3.3	.30	.77	-.55	-.03
1200	1	0	0	0	832	-.50	-.9	3.5	.29	.89	-.65	-.01
1500	1	0	0	0	664	-.44	1.1	3.7	.42	1.0	-.85	-.08
1700	1	0	0	0	616	-.50	1.3	3.9	.60	1.1	-1.2	-.04
1900	1	0	0	0	575	-.82	1.4	4.2	.70	1.4	-1.1	-.06
2000	1	0	0	0	1016	-.88	1.5	4.5	.70	1.5	-1.3	-.05
2200	1	0	0	0	450	-1.1	1.6	4.5	.80	1.5	-1.1	-.06
2400	1	0	0	0	419	-1.1	1.7	4.9	.90	1.8	-1.4	-.07
3000	1	0	0	0	403	-2.0	2.1	5.3	1.3	2.1	-1.3	-.10
4000	1	0	0	0	400	-1.8	2.0	5.0	1.3	2.1	-1.7	-.10

Table II. Correlation Coefficients

T	υ_{HH}	J_{HH}	υ_{OH}	J_{OH}	$\gamma_{r_1\upsilon_1}$	γ_{Tr_1}	$\gamma_{T\upsilon_1}$	$\gamma_{r_2\upsilon_2}$	γ_{Tr_2}	$\gamma_{T\upsilon_2}$	$\gamma_{r_1r_2}$	$\gamma_{r_1\upsilon_2}$	$\gamma_{\upsilon_1r_2}$	$\gamma_{\upsilon_1\upsilon_2}$
300	1	0	0	0	-.80	.18	-.55	-.16	-.66	.06	.33	.09	-.22	-.07
600	1	0	0	0	-.55	.28	-.73	-.15	-.18	-.01	.32	-.11	-.37	-.34
800	1	0	0	0	-.56	.15	-.71	-.15	-.10	-.06	.16	-.14	-.34	-.26
1000	1	0	0	0	-.60	.16	-.67	-.13	-.17	-.16	.22	-.22	-.34	-.10
1200	1	0	0	0	-.48	-.07	-.57	-.12	-.13	-.03	.30	.03	-.44	-.43
1500	1	0	0	0	-.45	.12	-.72	-.11	-.27	-.13	.25	-.20	-.27	-.21
1700	1	0	0	0	-.42	-.04	-.64	-.07	-.20	-.06	.13	-.13	-.34	-.34
1900	1	0	0	0	-.32	-.27	-.55	-.21	-.33	-.01	.30	-.10	-.34	-.33
2000	1	0	0	0	-.33	-.20	-.54	-.03	-.46	-.20	.18	-.02	-.22	-.30
2200	1	0	0	0	-.33	-.25	-.55	-.10	-.47	-.10	.23	-.11	-.21	-.27
2400	1	0	0	0	-.28	-.25	-.61	-.18	-.39	-.11	.22	-.09	-.25	-.21
3000	1	0	0	0	-.44	-.22	-.44	-.03	-.60	-.28	.10	-.02	-.10	-.23
4000	1	0	0	0	-.37	-.41	-.27	-.22	-.58	.09	.18	-.12	-.20	-.34

Table III. Reactive Trajectories								
T	v_{HH}	J_{HH}	v_{OH}	J_{OH}	RT	$\langle E_T \rangle$	$\langle J_{HOH} \rangle$	$\langle E_{HOH} \rangle$
600	1	0	0	0	201	12.2	10.1	31.2
800	1	0	0	0	201	12.2	10.4	31.7
1000	1	0	0	0	201	12.4	11.2	32.3
1200	1	0	0	0	201	13.5	10.1	31.7
1500	1	0	0	0	201	13.2	11.3	33.0
1700	1	0	0	0	201	13.4	12.1	33.4
1900	1	0	0	0	201	13.3	12.8	33.9
2000	1	0	0	0	402	14.3	12.5	33.4
2200	1	0	0	0	201	13.1	13.0	35.0
2400	1	0	0	0	201	13.7	13.3	35.0
3000	1	0	0	0	201	14.3	14.0	35.8
4000	1	0	0	0	201	14.7	14.1	37.3

Table IV. Non-Reactive Trajectories

T	v_{HH}	J_{HH}	v_{OH}	J_{OH}	NNR	$\langle\Delta E_T\rangle$	$\langle\Delta J_{HH}\rangle$	$\langle\Delta J_{OH}\rangle$	$\langle\Delta E_{r_{HH}}\rangle$	$\langle\Delta E_{r_{HH}}\rangle$	$\langle\Delta E_{v_{HH}}\rangle$	$\langle\Delta E_{v_{OH}}\rangle$
1200	0	0	0	0	965	-.66	.8	3.3	.23	.78	-.16	-.17
	1	0	0	0	832	-.50	.9	3.5	.29	.89	-.65	-.01
	2	0	0	0	644	-.25	1.1	3.3	.43	.77	-1.1	.16
	3	0	0	0	595	-.03	1.3	3.4	.78	.85	-1.7	.16
	4	0	0	0	567	-.05	1.4	3.4	.86	.90	-1.8	.12
1200	0	0	0	0	965	-.66	.8	3.3	.23	.78	-.16	-.17
	0	0	1	0	1071	-.81	.9	3.8	.29	1.1	-.06	-.47
	0	0	2	0	610	-.64	.9	3.8	.25	1.0	-.05	-.59
	0	0	3	0	602	-.78	.9	4.1	.30	1.3	-.08	-.88
	0	0	4	0	600	-.65	.9	4.2	.25	1.3	-.01	-.85
1200	1	0	1	0	889	-.47	1.0	3.7	.33	.96	-.49	-.32
2000	0	0	0	0	662	-1.6	1.4	4.6	.58	1.6	-.25	-.32
	1	0	0	0	1016	-.88	1.5	4.5	.71	1.5	-1.3	-.05
	2	0	0	0	381	-.70	1.6	4.1	.87	1.3	-1.8	.33
	3	0	0	0	353	-.27	1.8	4.2	1.2	1.3	-2.4	.14
	4	0	0	0	295	-.25	2.2	4.2	1.8	1.3	-3.0	.21
2000	0	0	0	0	662	-1.6	1.4	4.6	.58	1.6	-.25	-.32
	0	0	1	0	571	-1.4	1.4	4.7	.64	1.7	-.07	-.82
	0	0	2	0	565	-1.3	1.5	4.9	.70	1.8	.01	-1.2
	0	0	3	0	571	-1.2	1.4	5.2	.58	2.0	.08	-1.4
	0	0	4	0	529	-1.4	1.3	5.2	.59	2.1	.09	-1.3
2000	1	0	1	0	1334	-.87	1.6	4.6	.80	1.7	-.83	-.68

Table V. Correlation Coefficients

T	v_{HH}	J_{HH}	v_{OH}	J_{OH}	$\gamma_{r_1v_1}$	γ_{Tr_1}	γ_{Tv_1}	$\gamma_{r_2v_2}$	γ_{Tr_2}	γ_{Tv_2}	$\gamma_{r_1r_2}$	$\gamma_{r_1v_2}$	$\gamma_{v_1r_2}$	$\gamma_{v_1v_2}$
1200	0	0	0	0	-.33	-.14	-.36	-.37	-.32	-.44	.28	-.32	-.32	-.04
	1	0	0	0	-.48	-.07	-.57	-.12	-.13	-.03	.30	.03	-.44	-.43
	2	0	0	0	-.61	.28	-.71	.026	-.06	.14	.27	.00	-.36	-.53
	3	0	0	0	-.76	.34	-.71	.13	.10	.12	.17	.14	-.44	-.47
	4	0	0	0	-.70	.24	-.78	.02	.16	.14	.21	-.01	-.45	-.32
1200	0	0	0	0	-.33	-.14	-.36	-.37	-.32	-.44	.28	-.32	-.32	-.04
	0	0	1	0	.00	-.27	-.19	-.44	-.58	-.14	.29	-.43	-.16	.37
	0	0	2	0	-.11	-.09	-.13	-.40	-.28	-.45	.30	-.29	-.11	-.52
	0	0	3	0	.02	.01	-.08	-.62	-.36	-.24	.16	-.47	-.06	-.44
	0	0	4	0	-.04	-.12	-.08	-.51	-.38	-.37	.50	-.52	-.18	-.47
1200	1	0	1	0	-.48	.20	-.48	-.29	-.23	-.30	.16	-.18	-.19	-.39
2000	0	0	0	0	-.17	-.54	-.20	-.23	-.72	-.19	.34	-.14	-.15	-.24
	1	0	0	0	-.33	-.20	-.54	-.03	-.46	-.20	.18	-.02	-.22	-.30
	2	0	0	0	-.54	-.08	-.50	.05	-.32	-.06	.30	.04	-.31	-.52
	3	0	0	0	-.71	.14	-.63	.04	-.18	-.12	.18	-.06	-.34	-.23
	4	0	0	0	-.79	.11	-.50	-.01	-.27	.01	.22	-.01	-.29	-.32
2000	0	0	0	0	-.17	-.54	-.20	-.23	-.72	-.19	.34	-.14	-.15	-.24
	0	0	1	0	-.02	-.44	-.21	-.37	-.65	-.19	.35	-.37	-.06	-.32
	0	0	2	0	-.06	-.42	-.01	-.40	-.60	-.23	.31	-.30	-.06	-.51
	0	0	3	0	.01	-.20	-.08	-.47	-.44	-.30	.28	-.41	-.10	-.46
	0	0	4	0	.07	-.30	-.08	-.49	-.45	-.27	.19	-.35	-.03	-.50
2000	1	0	1	0	-.27	-.08	-.47	-.29	-.37	-.15	.16	-.31	-.24	-.33

Table VI. Reactive Trajectories

T	v_{HH}	J_{HH}	v_{OH}	J_{OH}	RT	$\langle E_T \rangle$	$\langle J_{HOH} \rangle$	$\langle E_{HOH} \rangle$
1200	0	0	0	0	201	13.4	10.8	20.5
	1	0	0	0	201	13.5	10.1	31.8
	2	0	0	0	169	12.0	12.5	44.6
	3	0	0	0	201	10.8	12.3	55.1
	4	0	0	0	201	10.0	13.5	64.8
1200	0	0	0	0	201	13.4	10.8	20.5
	0	0	1	0	196	14.6	10.5	29.8
	0	0	2	0	118	13.6	10.4	39.4
	0	0	3	0	96	13.3	9.7	47.9
	0	0	4	0	92	13.1	9.6	56.3
1200	1	0	1	0	201	12.9	10.8	42.3
2000	0	0	0	0	202	15.3	10.9	21.3
	1	0	0	0	402	14.3	12.5	33.4
	2	0	0	0	201	13.1	13.3	45.2
	3	0	0	0	201	12.6	14.2	55.8
	4	0	0	0	201	10.8	14.8	66.9
2000	0	0	0	0	202	15.3	10.9	21.3
	0	0	1	0	201	14.9	11.5	31.1
	0	0	2	0	136	14.7	11.4	40.5
	0	0	3	0	147	14.1	11.7	49.6
	0	0	4	0	144	14.0	11.1	57.9
2000	1	0	1	0	553	13.9	12.9	43.9

LIST OF FIGURES

13. The average energy in H_2O versus the initial vibrational energy of reagent molecules (kcal/mol) for ensembles at 1200 and 2000 K. Neither reagent molecule has rotational energy, and one reagent molecule had zero-point vibrational energy.

14. Histograms illustrating the distribution of the product translational energy (kcal/mol) in reactive collisions for the ensembles indicated.

15. Histograms illustrating the distribution of the product angular momenta ($\hbar$) in reactive collisions for the ensembles indicated.

16. Histograms illustrating the distribution of the product molecular energy (kcal/mol) in reactive collisions for the ensembles indicated.

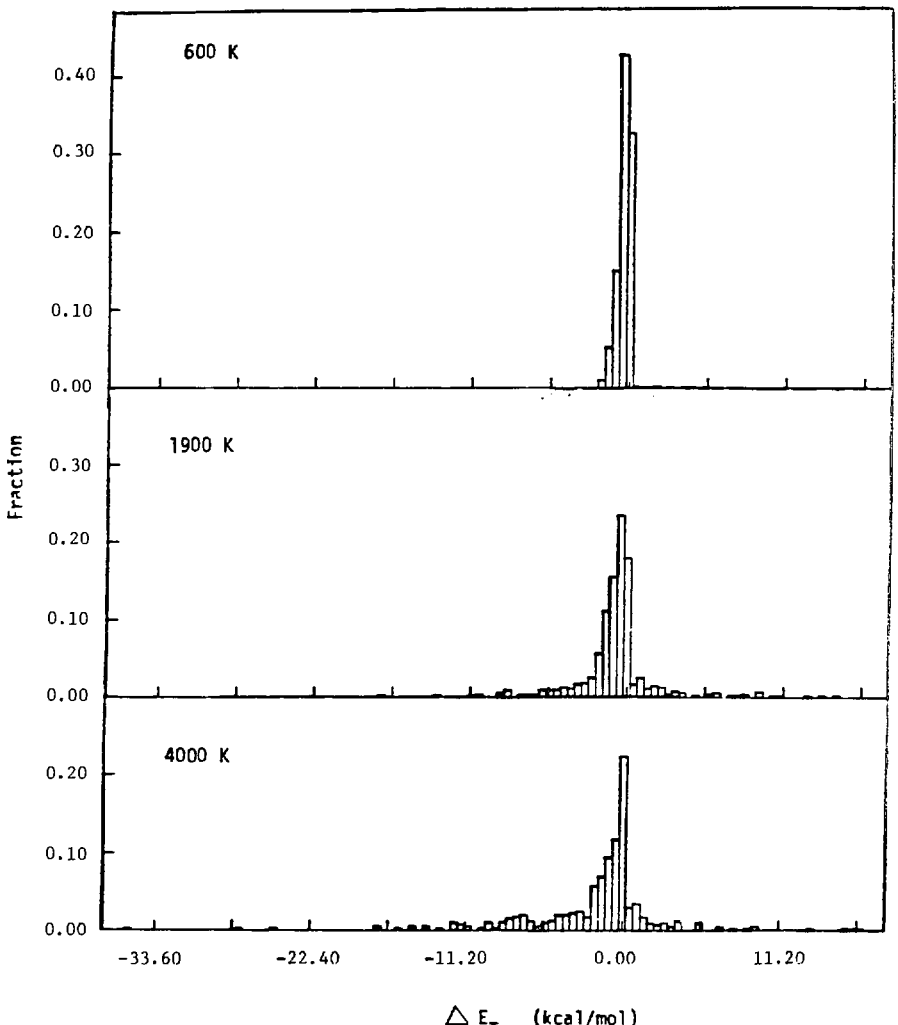
600 K
1900 K
4000 K
Fraction
0.40
0.30
0.20
0.10
0.00
-33.60
-22.40
-11.20
0.00
11.20
△ E_T (kcal/mol)

Fig. 1

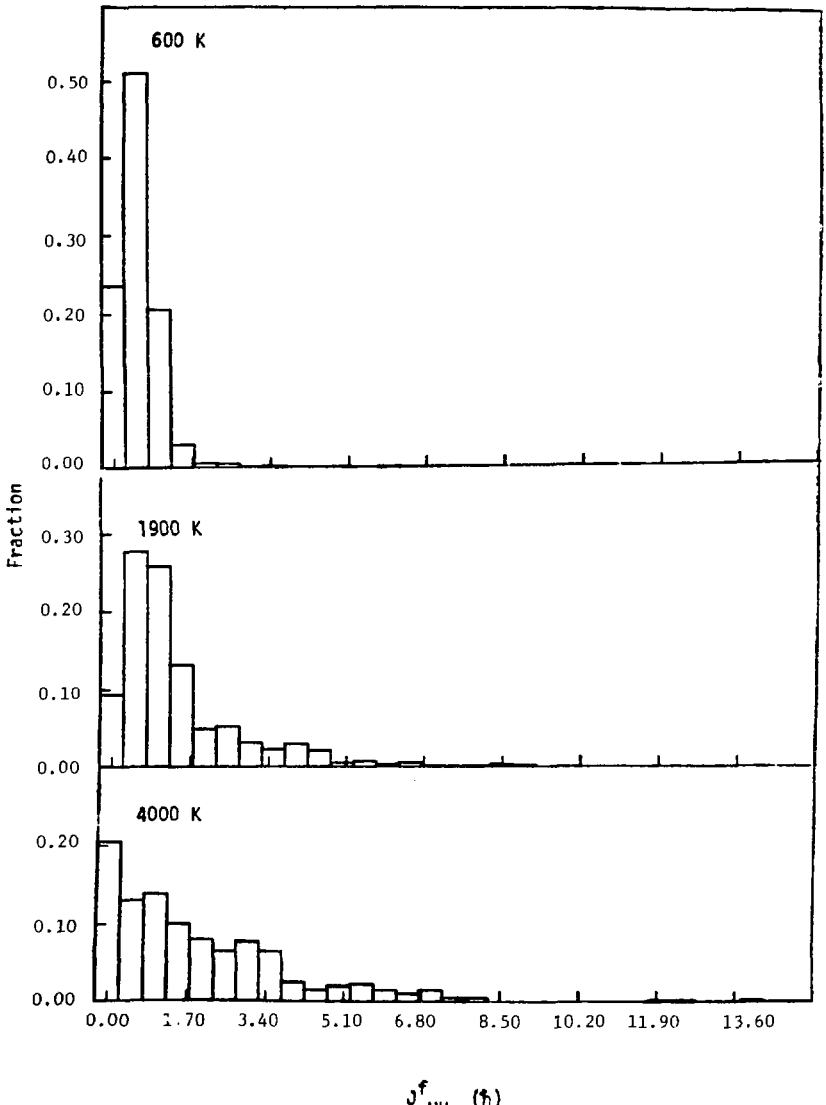
600 K
0.50
0.40
0.30
0.20
0.10
0.00
1900 K
0.30
0.20
0.10
0.00
4000 K
0.20
0.10
0.00
Fraction
0.00
1.70
3.40
5.10
6.80
8.50
10.20
11.90
13.60
J^f_{HH} (ħ)

Fig. 2

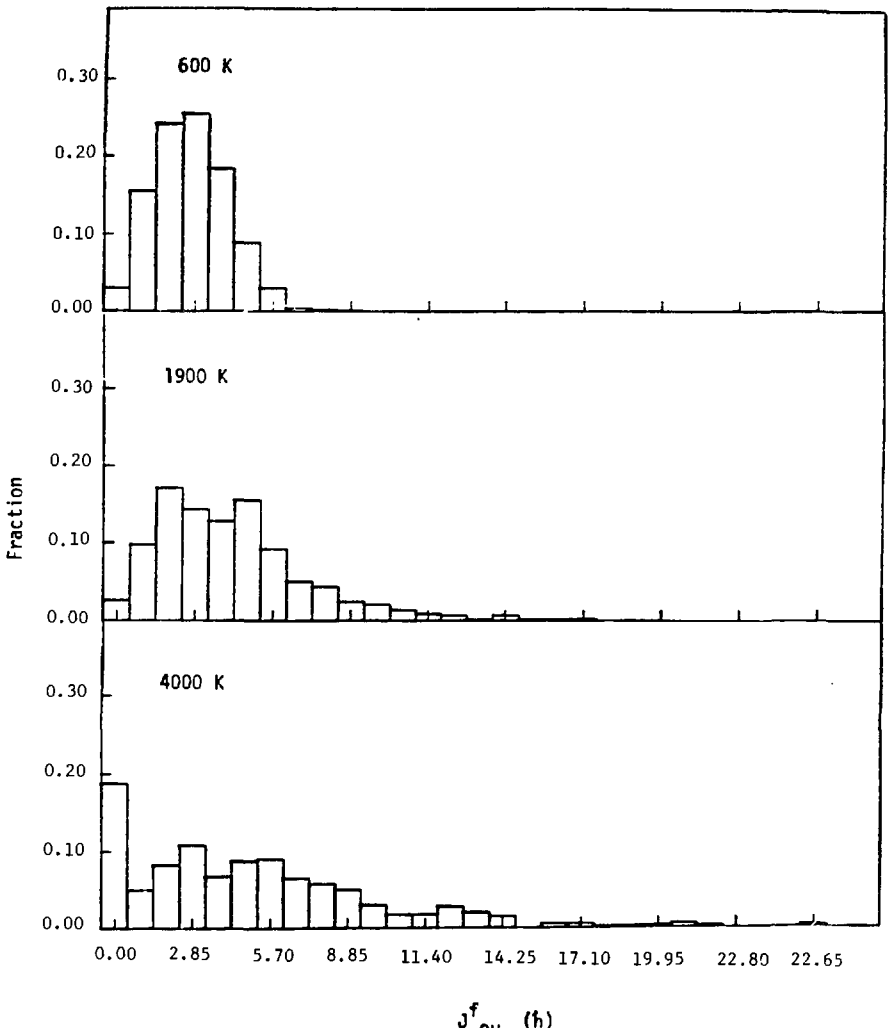
600 K
1900 K
4000 K
Fraction
0.30
0.20
0.10
0.00
0.00
2.85
5.70
8.85
11.40
14.25
17.10
19.95
22.80
22.65
J^f_{OH} (ħ)

Fig. 3

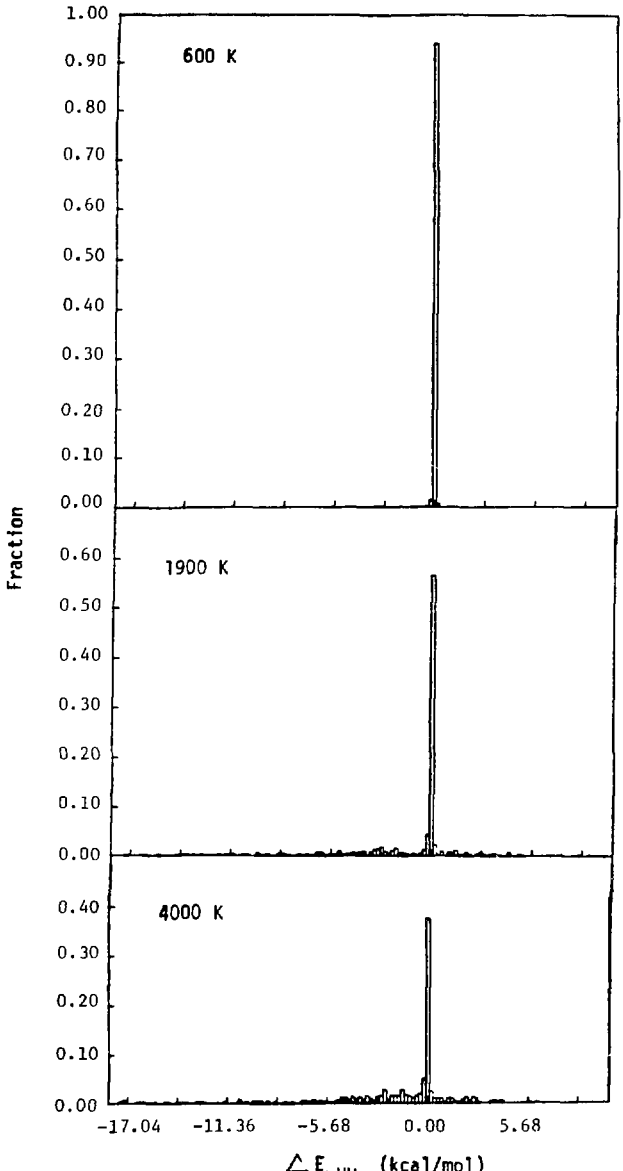
600 K
1900 K
4000 K
Fraction
1.00
0.90
0.80
0.70
0.60
0.50
0.40
0.30
0.20
0.10
0.00
0.60
0.50
0.40
0.30
0.20
0.10
0.00
0.40
0.30
0.20
0.10
0.00
-17.04
-11.36
-5.68
0.00
5.68
△ E_vHH (kcal/mol)

Fig. 4

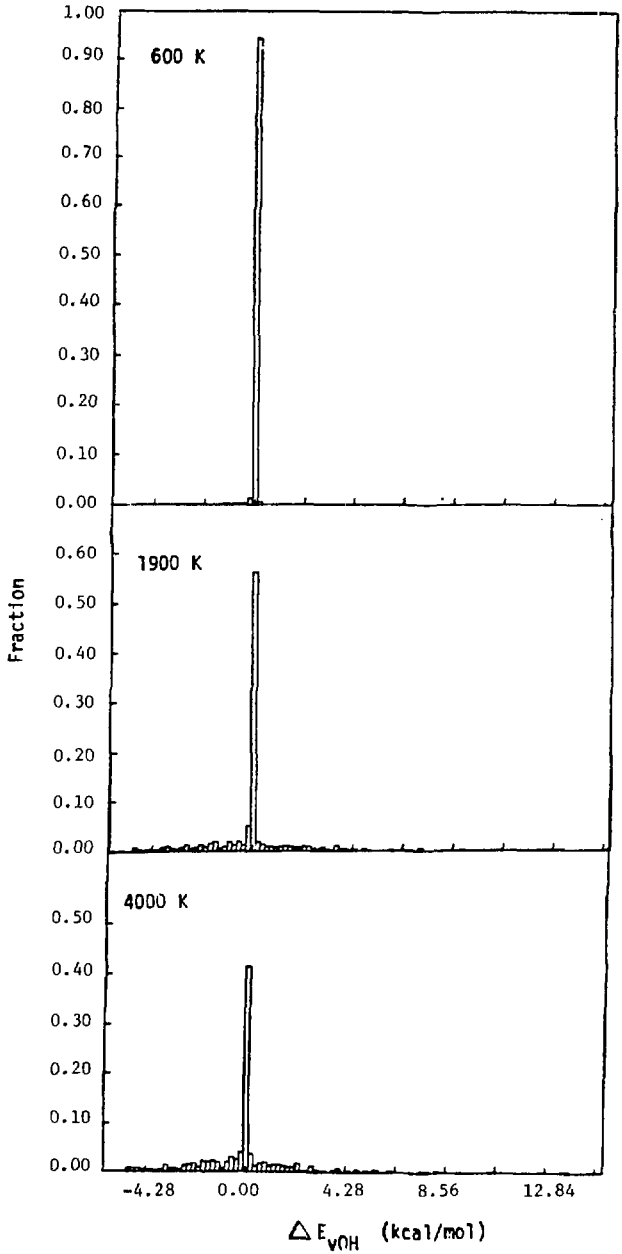
600 K
1900 K
4000 K
Fraction
1.00
0.90
0.80
0.70
0.60
0.50
0.40
0.30
0.20
0.10
0.00
-4.28
0.00
4.28
8.56
12.84
ΔE_vOH (kcal/mol)

Fig. 5

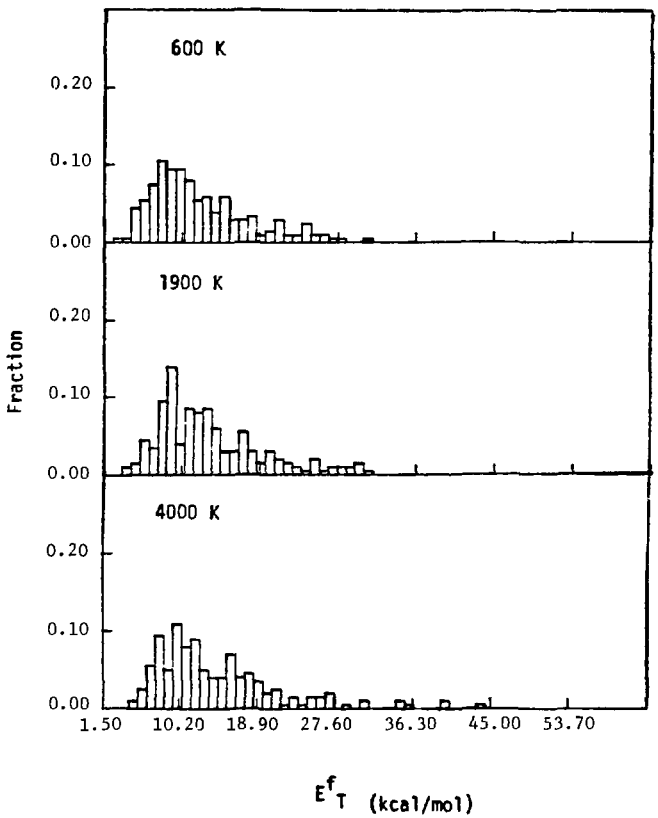
600 K
1900 K
4000 K
Fraction
0.20
0.10
0.00
1.50
10.20
18.90
27.60
36.30
45.00
53.70
E^f_T (kcal/mol)

Fig. 6

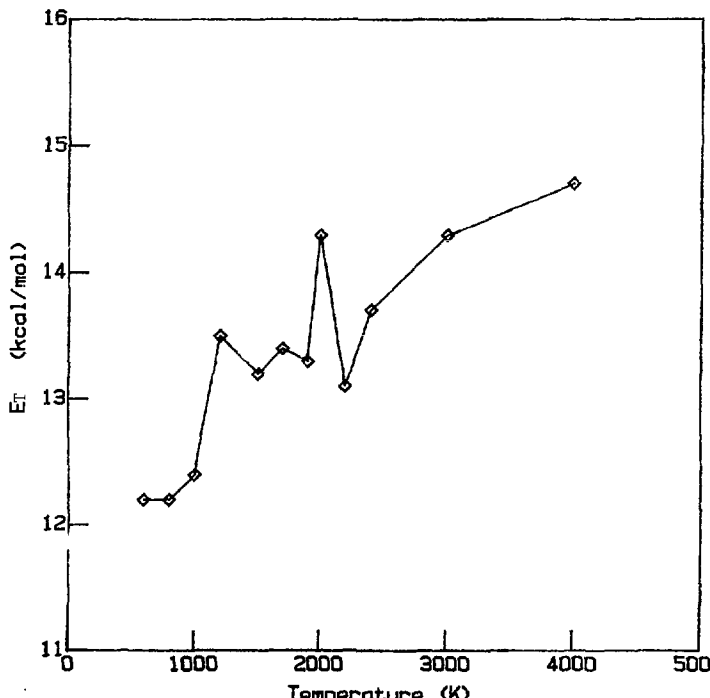
16
15
14
13
12
11
E_T (kcal/mol)
0
1000
2000
3000
4000
5000
Temperature (K)

Fig. 7

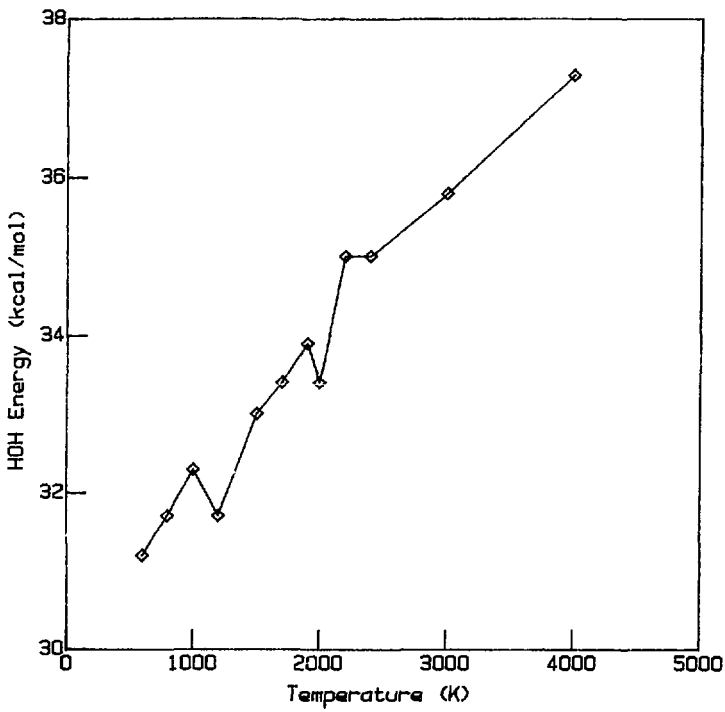
38
36
34
32
30
HOH Energy (kcal/mol)
0
1000
2000
3000
4000
5000
Temperature (K)

Fig. 8

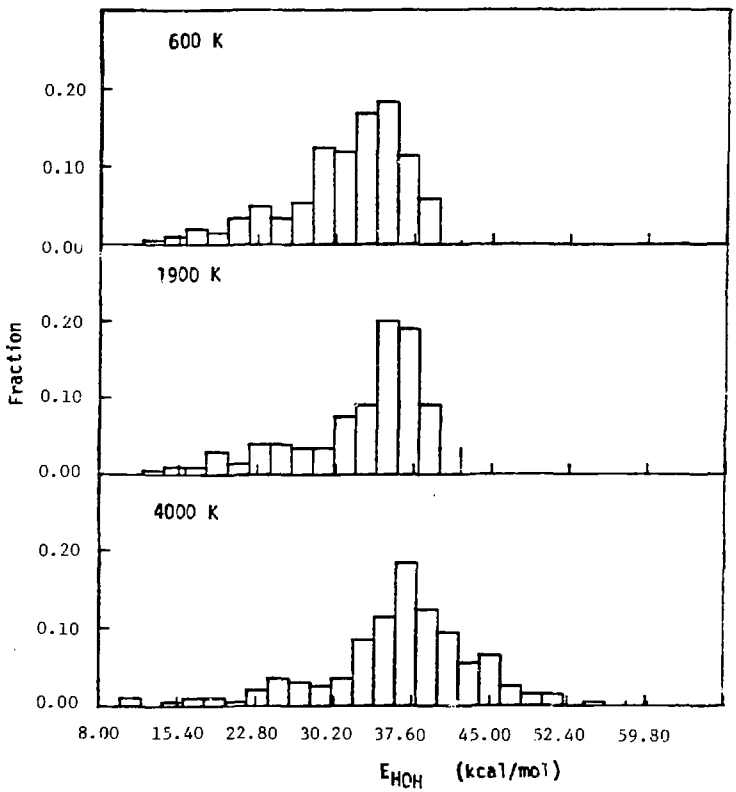
600 K
1900 K
4000 K
Fraction
0.20
0.10
0.00
8.00
15.40
22.80
30.20
37.60
45.00
52.40
59.80
E_{HOH} (kcal/mol)

Fig. 9

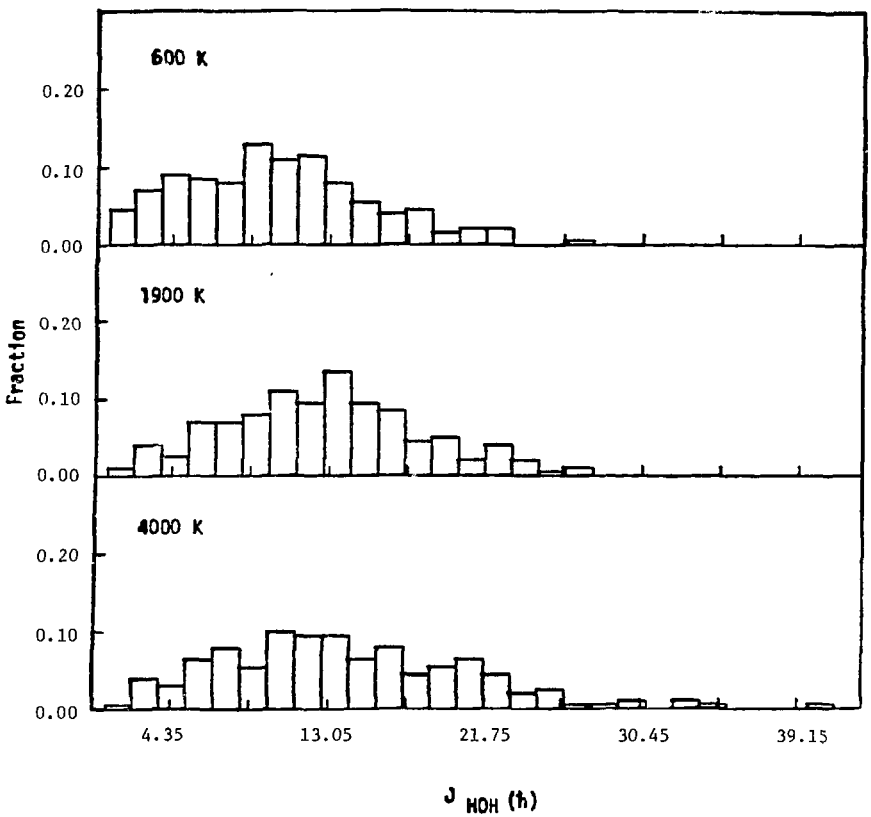
600 K
1900 K
4000 K
Fraction
0.20
0.10
0.00
4.35
13.05
21.75
30.45
39.15
J HOH (h)

Fig. 10

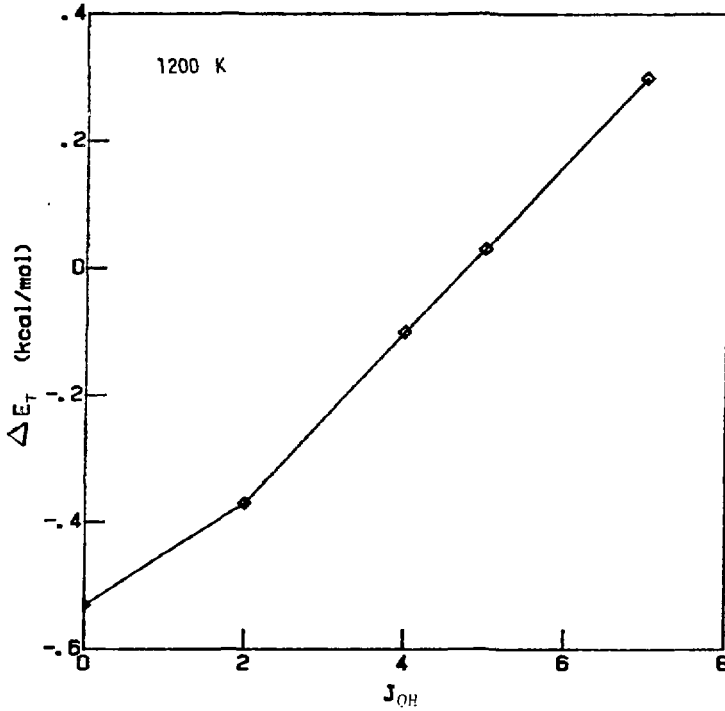

Fig. 11

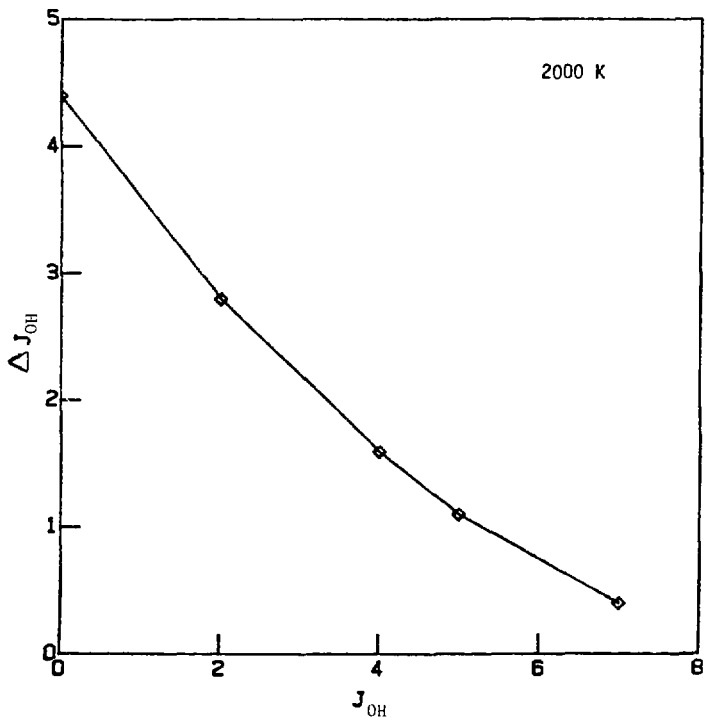

Fig. 12

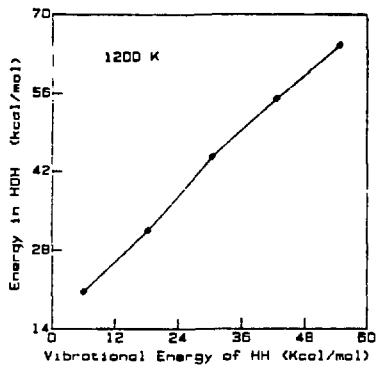
1200 K
Energy in HOH (Kcal/mol)
70
56
42
28
14
0
12
24
36
48
60
Vibrational Energy of HH (Kcal/mol)

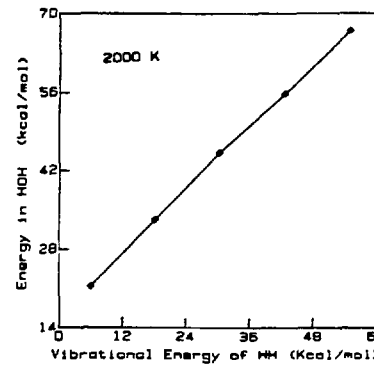
2000 K
Energy in HOH (Kcal/mol)
70
56
42
28
14
0
12
24
36
48
60
Vibrational Energy of HH (Kcal/mol)

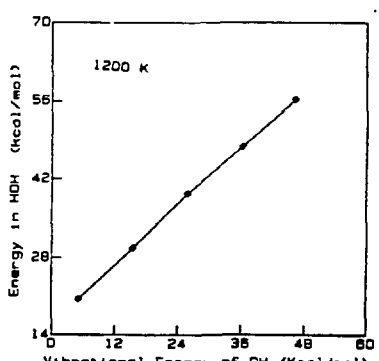
1200 K
Energy in HOH (Kcal/mol)
70
56
42
28
14
0
12
24
36
48
60
Vibrational Energy of OH (Kcal/mol)

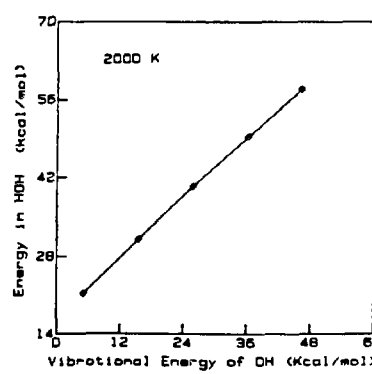
2000 K
Energy in HOH (Kcal/mol)
70
56
42
28
14
0
12
24
36
48
60
Vibrational Energy of OH (Kcal/mol)

Fig. 13

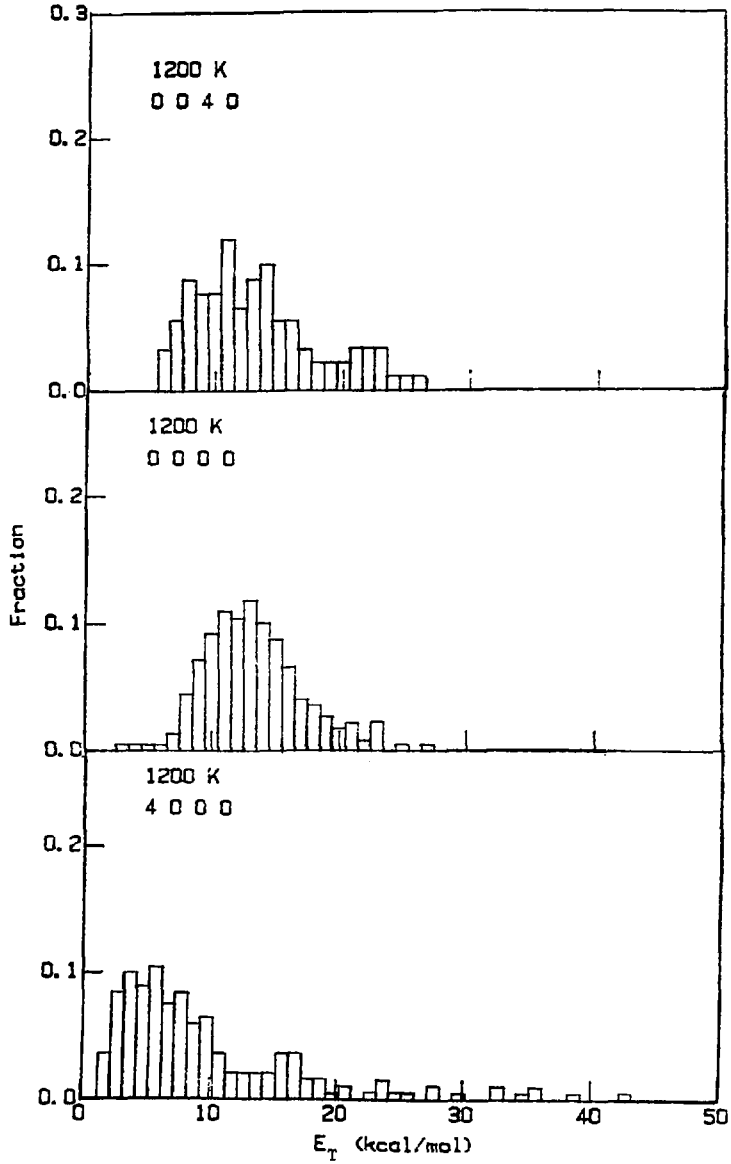
1200 K
0 0 4 0
1200 K
0 0 0 0
1200 K
4 0 0 0
Fraction
0.3
0.2
0.1
0.0
0
10
20
30
40
50
E_T (kcal/mol)

Fig. 14

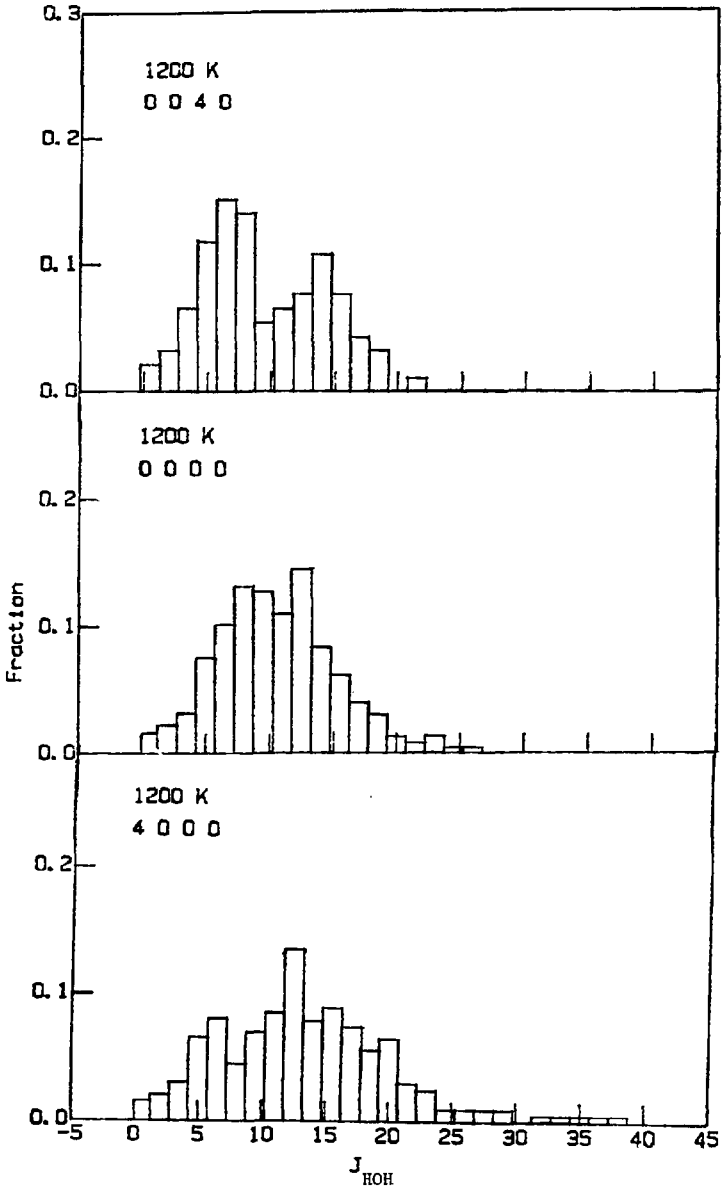
1200 K
0 0 4 0
1200 K
0 0 0 0
1200 K
4 0 0 0
Fraction
0.0
0.1
0.2
0.3
-5
0
5
10
15
20
25
30
35
40
45
J HOH

Fig. 15

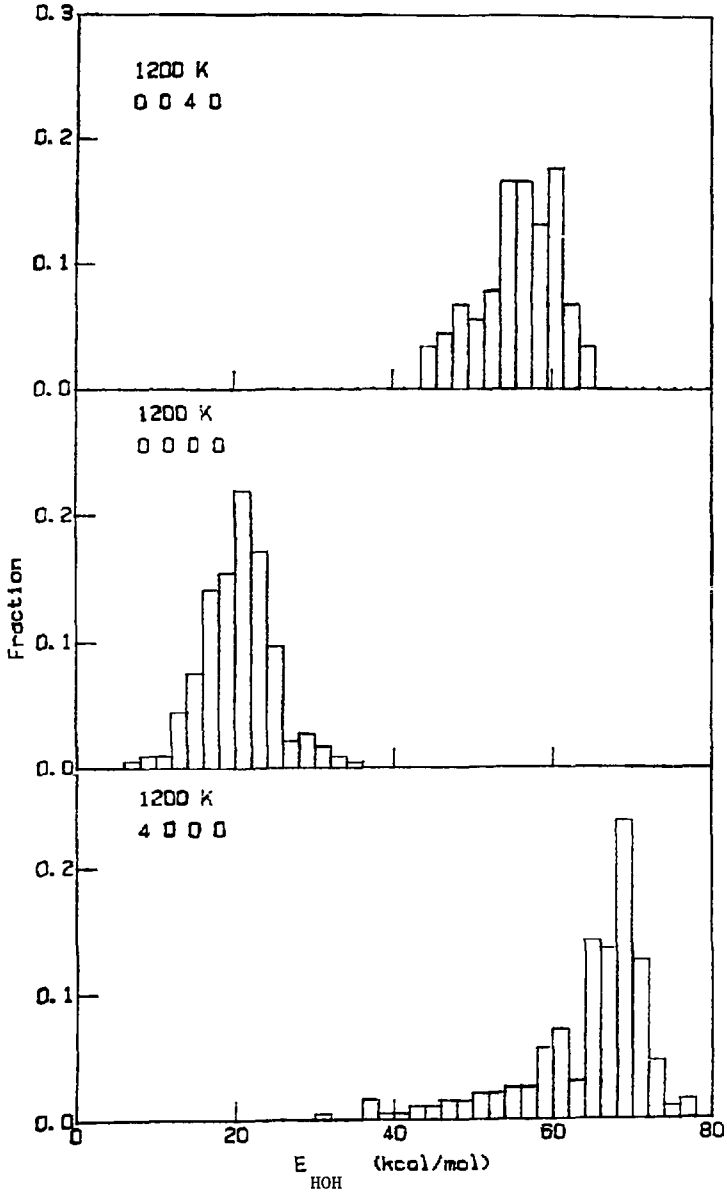
1200 K
0 0 4 0
1200 K
0 0 0 0
1200 K
4 0 0 0
Fraction
0.3
0.2
0.1
0.0
0
20
40
60
80
E HOH (kcal/mol)

Fig. 16